A Multistage Passive Islanding Detection Method for Synchronous-Based Distributed Generation

***Abstract*—A multistage approach to passive islanding detection is proposed that utilizes a decision-tree-like classification algorithm. The novelty of the proposed method is centered on the way in which features are passed to subsequent stages of the decision tree (DT). Feature sets extracted using different sized time windows are passed to successive stages of the tree. This provides two important advantages: (i) cases which can be easily determined as either islanding or non-islanding events are flagged as soon as possible without waiting for the full feature set to become available (ii) because the algorithm allows for the use of different sized time windows, features are analyzed in time-scales which fit their natural patterns of temporal evolution. The proposed classifier is trained and tested using a database of feature vectors, obtained using PSCAD, which were designed to reflect a variety of commonly encountered events on an IEEE 34-bus distribution system. One of the key requirements for the proposed algorithm was that easy cases should be flagged as soon as possible; this property was confirmed by the observation that most events (≈79%) were detected within 10-20ms, while at the same time retaining a very high detection rate overall cases (>99%).**

***Index Terms*—Islanding detection, non-detection zone, decision tree, distributed generation.**

I. Introduction

ISLANDING detection can be conducted locally at the point of common coupling (PCC) or remotely at the utility side by means of advanced communication techniques. Local methods can generally be grouped into active and passive methods depending on their operating mechanism [1]. When the detection method fails to identify an islanding case within the preset time limit, the incident event is said to fall within the non-detection zone (NDZ) of the method [2]. Many research efforts have focused on reducing the size of the NDZ in active schemes by carefully setting the thresholds on various parameters [3].

An active method operates by intentionally injecting perturbations into the grid at the PCC and then relies on the main utility to maintain the system in a stable state. Active schemes are deemed to have smaller NDZs compared to passive schemes [2]. The main disadvantage of active schemes is the instability introduced by the injected perturbations and the subsequent degradation of power quality [4].

In contrast, a passive detection scheme uses only the measurements made at the PCC. A relay equipped with a passive detection algorithm observes various local measurement parameters then makes the decision to trip based on predefined thresholds. Typical passive methods include over/under voltage and over/under frequency protection (OVP/UVP and OFP/UFP) [5], the rate of change of system parameters like frequency [6], rate of change of active power [7], rate of change of phase angle difference [8], and the rate of change of frequency with power [9]. The change in voltage angle has also been used as a parameter in vector surge relays [10]. The use of the voltage unbalance to detect islanding was studied in [11]. More sophisticated signal processing techniques such as the discrete wavelet transform and S-transform have also been applied to achieve faster detection [12]. In summary, both passive and active approaches have their respective advantages and disadvantages. In this paper, our focus is on the use of intelligent algorithms for islanding detection, which tend to be more relevant to passive detection methods. However, it is not our intention to argue that one approach is superior to the other.

A. Literature Review

The application of intelligent and machine learning algorithms in detecting islanding events is described in [13] - [21]. For example, the research work in [13] proposes the use of the naïve-Bayes classifier to classify the coefficients extracted from applying estimation of signal parameters via rotational invariant technique. Even though this method resulted in a good classification accuracy, it is limited to a single time window of 100ms duration. In [14], a fast gauss-Newton algorithm was presented for the islanding detection problem, which works in recursive and decoupled manner. In [15], a decision tree (DT)-based approach which used 11 features was proposed for use with a system with synchronous-based DG. The decision-making times were in the range of 45 to 50 ms, and the mis-classification rate was 0% for non-islanding events and 16% for islanding events. The work in [16] presented a comparison between using three classifiers: DTs, support vector machines (SVM) and probabilistic neural networks for islanding detection. The classifiers were trained using features extracted at a fixed time window size after applying discrete wavelet transform to extract features. The results showed that the DT classifier achieved the highest classification accuracy of the three, at 80%.

In [17], features including positive and negative sequence quantities are extracted using discrete Fourier transform and a decision tree is trained to build the data mining model for islanding detection. In [18], a multi-feature SVM-based classifier is proposed for islanding detection. In [19], autoregressive signal modeling is utilized to extract signal features which are then passed to an SVM classifier for detecting islanding conditions. In [20], signal features are extracted using hyperbolic S-transform, time-domain transform and mathematical morphology methods and similarly SVM is implemented to distinguish islanding from other power quality events. In [21], wavelet is used to extract features and machine learning algorithms are implemented to automate the classification process.

https://doi.org/10.1109/TII.2021.3065015

The use of SVM as a dual-functional classifier for detecting and discriminating islanding against grid-connected mode and grid fault against the normal condition is proposed in [22]. In [23], a method that relies on adaptive neuro-fuzzy inference system is proposed where seven parameters are monitored at the DG point of common coupling and it has been shown that the proposed method will depend on the sampled time as well as the number of samples.

B. Contribution and Paper Organization

A common feature of the examples listed above is that they are based on feature vectors that are derived from time windows of uniform length. While this assumption simplifies the feature extraction and classification process, it is certainly not a self-evident fact. As a counterpoint, we put forward the following two postulations:

1) Many commonly encountered power system events are simple in that they can be easily classified as either islanding or non-islanding occurrences. If this is true, then it should be possible to quickly identify and flag these events accordingly, thus avoiding unnecessary delays in the decision-making process.
2) The temporal evolution of islanding-related features occur over different time scales. As such, extracting features from uniformly sized time windows is akin to taking a "one-size-fits-all" approach. If this is true, then using variable-sized time windows may result in higher accuracy rates compared to traditional methods.

All aforementioned islanding detection methods relying on feature extraction, utilize one window size for determining the features as well as their thresholds to be utilized for islanding detection. The features extracted will depend on the time window size (sampled time) as indicated in [23]. Thus, the main contribution of this paper is developing an islanding detection method with minimal NDZ while achieving fast detection by utilizing a multi-stage multi-window approach where in each time window (stage) the optimal features and their thresholds are determined.

In this paper, we seek to demonstrate the validity of these two statements by developing and testing a novel, multi-stage islanding detection method on a system incorporating synchronous-based DG. The proposed method is based on a *decision tree-like* (DTL) algorithm that operates on features derived from a series of time windows of increasing length. While traditional DTs use a single stationary set of features, the approach presented uses features extracted from the different time windows as input to successive stages in the tree.

The proposed approach is tested on the standard IEEE 34-bus radial distribution system that is modeled using PSCAD/EMTDC software. A comprehensive training database that covers a wide variety of loads, real and reactive power mismatches and different scenarios encompassing both islanding and non-islanding events has been generated and is used to train and test the DTL classifier. For a given DG capacity, the active and reactive power mismatch is adjusted by varying the load resistance, inductance and capacitance to achieve the desired percentage mismatches in active and reactive power at the DG PCC. Finally, the results obtained for different sets of training and testing data sizes are compared.

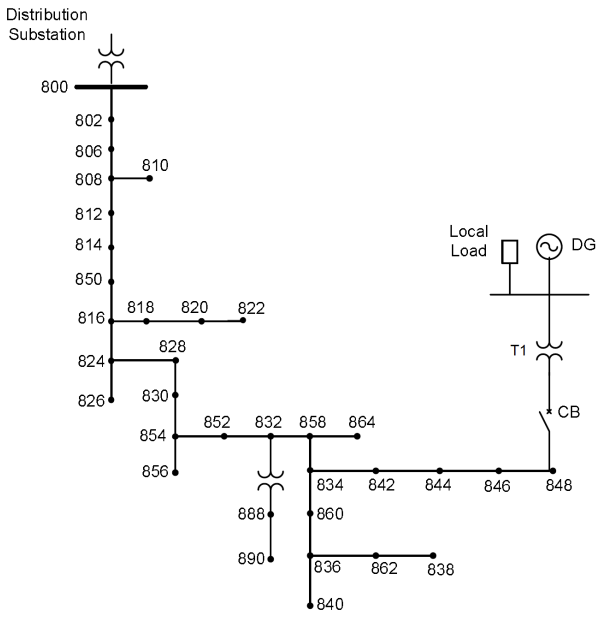

Fig. 1. IEEE 34-Bus System with a synchronous-based DG unit

II. System Modeling and Simulations

In this study, the IEEE 34-bus distribution network with synchronous-based distributed generator (DG) is modeled using PSCAD/EMTDC simulations. A set of events corresponding to islanding and non-islanding cases are simulated using various loading conditions at different locations. Sixteen features were extracted based on the values of voltage, power and frequency measured at the PCC. For real-time implementation for the proposed algorithm, system parameters (for example, frequency and voltage) will be continuously monitored and the first stage of the algorithm will be triggered at the moment when any noticeable deviation is detected in such parameters.

A. System under study

A schematic of the IEEE 34-bus distribution network is shown in Fig. 1. The distribution system is connected with the grid through a 69kV/24.9kV transformer. A synchronous-based DG rated for 1MVA, operating at unity power factor, is connected at node 848 through a 24.9 kV/6.6 kV transformer. This DG is equipped with an IEEE Type-1 exciter model. In distribution systems, loads can vary from constant power loads to loads that are voltage and frequency dependent. It has been shown, in [19] and [24], that the load type can have an impact on the islanding detection capability and thus it is important to consider the load voltage and frequency dependence when analyzing islanding detection. Loads modeled in this system are of the static type load model mentioned in [25]. The mathematical representation of the static load characteristics is as follows:

$$P = P_0 \left(\frac{V}{V_0}\right)^{NP} (1 + K_{pf}\Delta f) \quad (1)$$

$$Q = Q_0 \left(\frac{V}{V_0}\right)^{NQ} (1 + K_{qf}\Delta f) \quad (2)$$

TABLE I
SUMMARY OF SIMULATED EVENTS

Event description	Number of events	Event class
RLC loads with active and reactive power mismatch	5,906	islanding
Single-phase short circuit at various locations	620	non-islanding
Three-phase short circuit at various locations	628	non-islanding
Capacitor switching at various locations	1,260	non-islanding
Load switching at various locations	3,151	non-islanding
Non-linear load switching at various locations	800	non-islanding
Motor switching at various locations	630	non-islanding

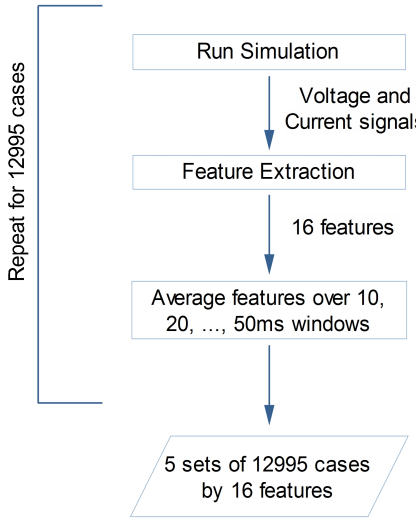

Fig. 2. Detailed steps involving dataset generation

where V_0, P_0, and Q_0 are the nominal load's voltage, active, and reactive power respectively. Δf is the deviation in frequency from the rated value $(f - f_0)$. NP and NQ have values between 0 and 2 which determine the load's characteristic (constant power, constant current or constant impedance when the values are 0, 1, or 2 respectively). The constants K_{pf} and K_{qf} shape the load's response for frequency deviation [25].

In addition to load variation, two system loading conditions are considered: normal and reduced system loading; the latter was simulated by disconnecting the link between nodes 834 and 860, which removes all subsequent loads.

B. Simulated cases

Table I summarizes the simulated events. As can be seen, two major categories of events were simulated, namely "islanding" and "non-islanding". IEEE Standard 1547 mandates that the detection method be tested on various mismatches between the power generated and the demands of these local loads. To satisfy this requirement, a variety of local load combinations were simulated for the islanding cases by controlling the real and reactive power mismatches within the range from 0% to 15%.

For the non-islanding category, disturbances that may occur during the normal operation of the system were simulated. Hence, five main types of non-islanding events have been simulated: (1) Single and three-phase short circuit faults taking place at various locations and lasting for 100ms before being cleared; (2) Capacitor switching events at various locations with total capacity of 12.29 μF, 8.29 μF and 5.29 μF; (3) RLC loads rated between 0.3MW and 1.4MW switching events at various locations and different power factors from 0.90 to 0.98; (4) Non-linear load switching; and (5) Induction motor switching at different locations. The variations in capacitor as well as load values have been chosen such that the voltage levels are within the IEEE Std. 1547 threshold values during normal operating conditions [26]. In summary, a total of 7089 non-islanding and 5906 islanding events were generated, as is shown in table I.

Voltage and frequency waveforms measured at the PCC during islanding events at various active power mismatch conditions are shown in Fig. 3, while the corresponding waveforms for non-islanding events related to load switching, capacitor switching, single and three-phase short circuits are shown in Fig. 4. It can be clearly seen that the islanding event has minimal deviation and is hence not detectable using OVP/UVP or OFP/UFP protective relays. Hence, more intelligent islanding detection methods are required when DG units are involved.

C. Feature extraction

Fig. 2 shows the detailed steps involved in dataset generation. Feature vectors corresponding to the simulated events are extracted from measurements made at the PCC. Features are extracted using sliding windows of 10ms, 20ms, ... , 50ms in length and are then stored in five different matrices along with the target vectors as shown in the figure. In this paper, in addition to voltage symmetrical components, features for islanding detection were selected based on available features used in [10], [15], [27]- [30]. During an islanding event, there could be excess or deficit generation capacity in the islanded system. Such a mismatch between the generation and load will result in changes in both voltage and frequency which in turn will impact the active and reactive power generated by the DG. For this reason, such parameters in addition to their rate of change could be effective in distinguishing an islanding event. Furthermore, transients generated after an islanding event on a three-phase system are unbalanced due to the time shift in the opening of the breaker poles on each phase (the breaker poles open at the current zero-crossing) which thus affect the voltage symmetrical components magnitude as well as THD.

In this study, the following features are considered as potential predictors of islanding: DG units active and reactive power P and Q, rated voltage V, terminal frequency F, the negative, positive and zero-sequence voltage components V_-, V_+, and V_0, and the total harmonic distortion of voltage THD_V. The Fast Fourier Transform and symmetrical component transformation block in PSCAD/EMTDC was utilized for determining the value of THD and sequence components.

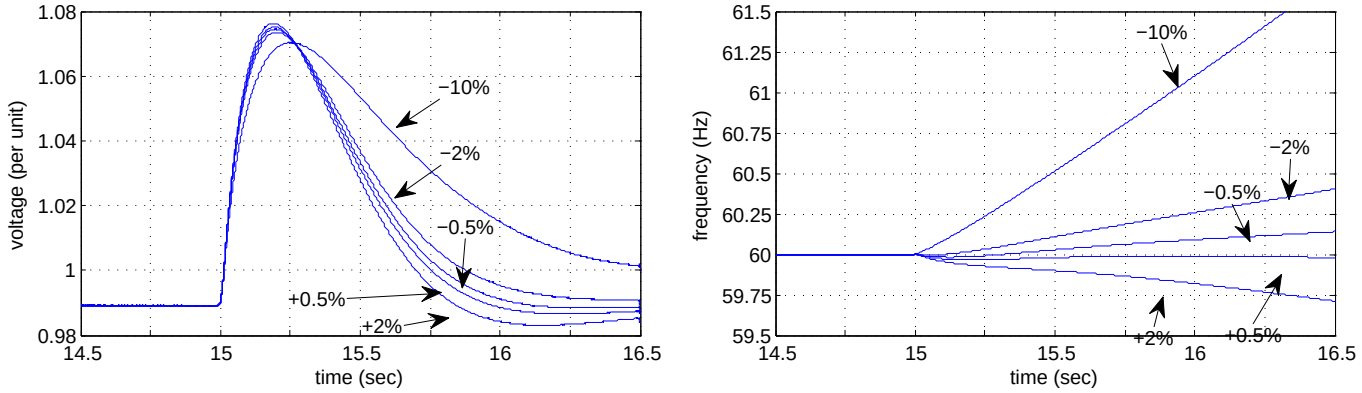

(a) (b)

Fig. 3. (a) System voltage and (b) frequency waveforms at PCC due to a islanding event occurred at 15.0s for the following mismatches in active power supplied: -10%, -2%, -0.5%, +0.5%, and +2% while the system is carrying an RLC load with a power factor of 0.98 supplied by a single DG at bus 832

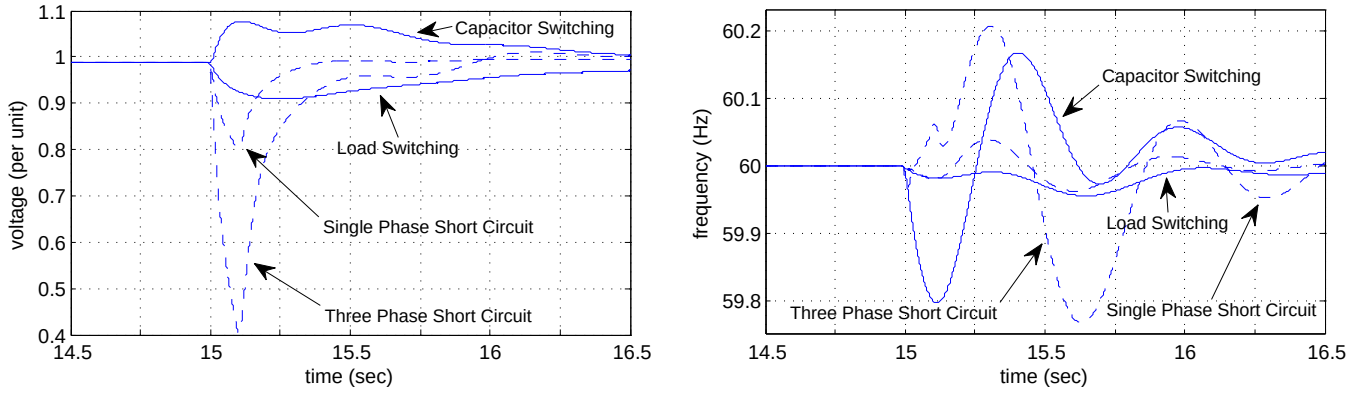

(a) (b)

Fig. 4. (a) System voltage and (b) frequency waveforms at PCC due to disturbances (non-islanding events) occurred at 15.0s at the bus 812.

TABLE II
LIST OF THE POTENTIAL FEATURES COLLECTED AT THE PCC

V	F	P	Q	V_-	V_+	V_0	THD_V
δV	δF	δP	δQ	δV_-	δV_+	δV_0	δTHD_V

$$THD_V = \frac{\sqrt{V_2^2 + V_3^2 + \cdots + V_h^2}}{V_1} \tag{3}$$

where h is the number of harmonics and V_i is the voltage magnitude of the i^{th} harmonic order.

In addition to the above features, the derivative of each signal has been also included in the set of features. Derivatives were estimated by splitting the respective time window into two parts then taking the difference between the average of each part divided by the total window size. For example, the derivative of a feature K is calculated as shown in Eq. (4) below:

$$\delta K = \frac{2}{n}\left(\sum_{i=1}^{n/2} K_i - \sum_{i=n/2+1}^{n} K_i\right)/w \tag{4}$$

where n is the number of samples taken in the given time window, w is the window size in seconds, and K_i is the i^{th} sample of the feature K. The set of features considered in this study is provided in Table II.

III. TRAINING THE DTL CLASSIFIER

The proposed method consists of multiple classification stages that act on features extracted from time windows of different lengths. At each stage, events falling outside the pre-set decision boundaries are classified as either islanding or non-islanding, while events that fall within the boundaries (i.e. the NDZ of that stage) are passed to successive stages. So the problem of training the DTL classifier translates to (1) the process of identifying the optimal feature (or features) to be used in each stage and (2) setting the respective thresholds and associating these with the correct class labels.

It would be possible to conceive a variety of schemes for performing these operations, but whatever the exact algorithm used, it should be designed to reduce the overall classification time by minimizing the number of events falling within the NDZ at each stage. For this study, a greedy training algorithm was designed which explicitly satisfied the above requirement. As will be seen, the proposed algorithm is easy to implement, yet resulted in a very efficient performance.

Input to the training algorithm is a data of training samples having their features sampled at different time windows (stages) while the output is a decision tree made of the features that are the most informative at each stage associated with their thresholds values and recommended class labels. The first step in the algorithm, considering two features per stage, is to iden-

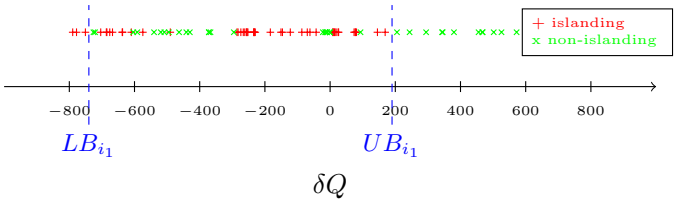

Fig. 5. Setting the upper and lower bounds for δQ at label switching points

tify the best combination of two features which can classify most of the training samples, whereas the remaining samples will be classified during the subsequent stage. Assuming the algorithm is evaluating the pair of features δQ and THD_V respectively, initially all training samples are sorted ascending on δQ values along with their class labels. The first switch in class label, i.e. from islanding to non-islanding or vise versa, denotes the threshold value of the lower boundary $LB_{\delta Q}$. Then training samples are sorted descending on δQ values and the first switch in class label will denotes the threshold value of the upper boundary $UB_{\delta Q}$ as explained in Fig. 5. In a similar way, the method evaluates the other feature THD_V, but after excluding the training samples having their δQ below $LB_{\delta Q}$ or above $UB_{\delta Q}$ from the training samples which produces LB_{THD_V} and UB_{THD_V}. Finally, features combination with lowest number of remaining unclassified samples is selected in the particular stage and the algorithm continues to the next stage until all the training samples are classified.

Note that having the training data presented as a set of feature matrices corresponding to different window sizes reflects the present situation where features extracted using shorter time windows will be available sooner, while features which require longer time windows will only be used later if required.

For a new data sample, classification is performed as follows: the value of the feature in the head of DT is compared against the lower and upper boundaries. If this value is within the boundaries LB and UB of that feature, comparison moves on to the second feature in the tree. Otherwise if the value is less than LB or above UB, the label associated with the particular boundary will be recommended as a predicted class label for the new sample.

IV. Results and Discussion

The proposed algorithm is implemented in Matlab and tested on the feature dataset extracted from the results of the IEEE 34-bus PSCAD simulation. The mechanism by which the proposed islanding detection approach discriminates between different kinds of events can be visually depicted using the NDZ graph. At each stage, the selected features progressively eliminate successfully classified subsets, while the remaining unclassified cases are passed on to subsequent stages and the procedure is repeated. This is illustrated in Fig. 6 where it can be seen that islanding events falling within region A cannot be correctly classified using only bounds on the two features THD_V and δQ. Thus, an event falling into that area will be passed to the next stage where a new set of feature bounds has to be identified. For the case where two features are used in each stage, the complete list of selected features along with the corresponding lower and upper thresholds are shown in

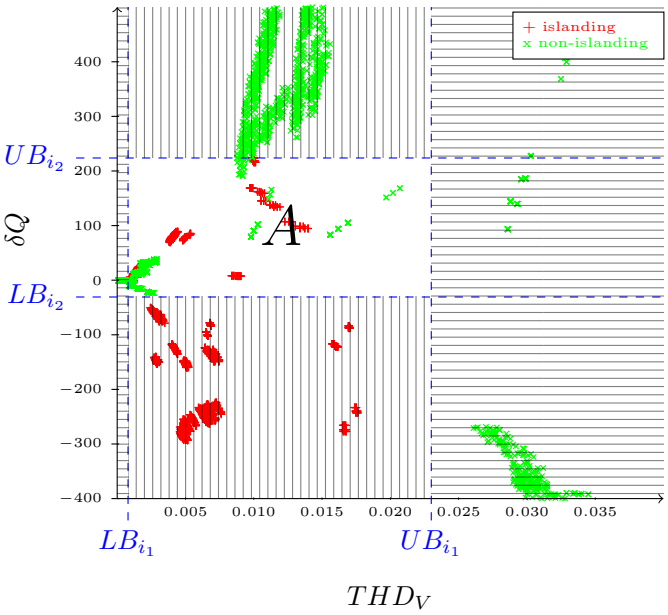

Fig. 6. Lower and upper bounds of THD_V and δQ. Islanding and non-islanding cases outside the bounds are detected, while area A is a NDZ.

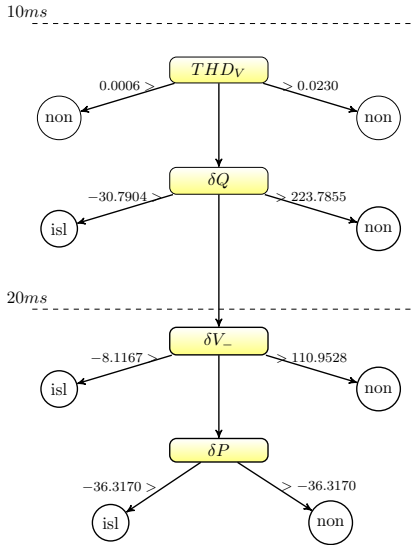

Fig. 7. A DTL classifier uses multiple time windows to detect islanding. (label "non" and "isl" denotes the non-islanding and islanding events)

Fig. 7 as a decision tree. The labels *non* and *isl* denote the non-islanding and islanding events respectively.

As can also be seen in Fig. 7, two separate collections of features are used, the first is extracted from the $0-10ms$ time window and the second from the $10-20ms$ time window. From this figure, it can be seen that some decisions are made after $10ms$ while others are deferred to the $20ms$ point. As explained earlier, this segregation of the data set into different stages allows for "easier" cases to be detected much sooner ($10ms$) while decisions on more difficult cases will be postponed until more information becomes available.

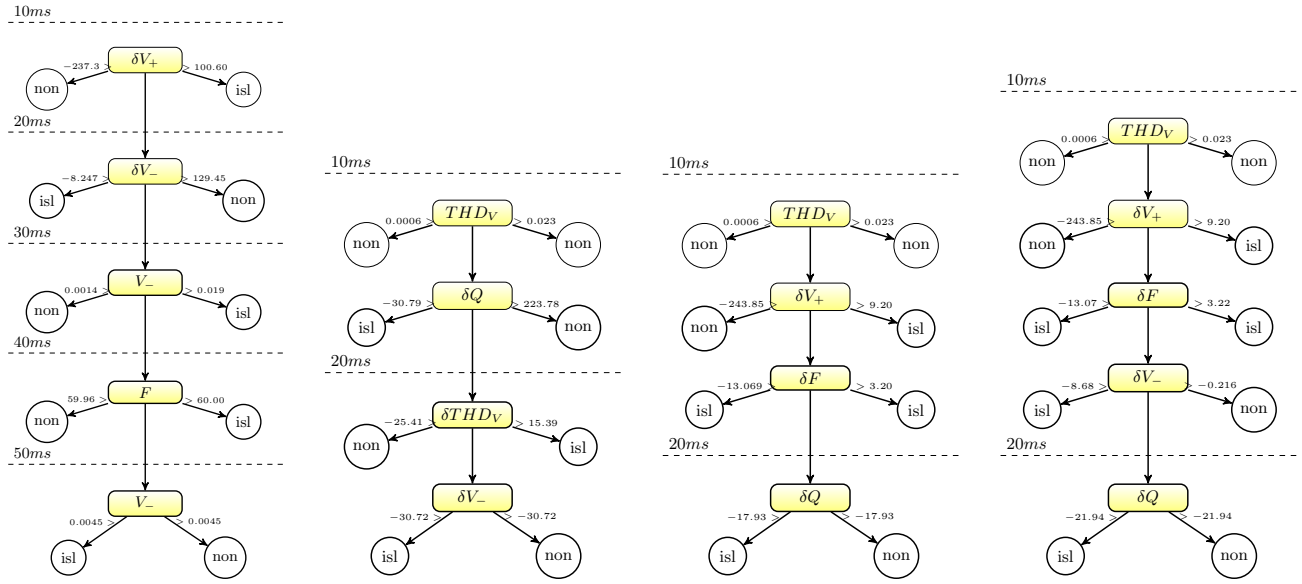

(a) one-feature per stage (b) two-features per stage (c) three-features per stage (d) four-features per stage

Fig. 8. Decision trees for feature sets of size M = 1, 2, 3, and 4 per stage

A. *Case I: Feature set size*

DTL classifiers using feature subsets of size $\{1, 2, 3, 4\}$ were trained then tested using data sets corresponding to time windows ranging from $10ms$ to $50ms$. The database is randomly divided using stratified sampling into two segments: 6,500 cases which were used to train the model, and a further 6,495 cases which were reserved for testing.

Feature sets are ranked based on the number of training events excluded by the feature thresholds. Table III shows the top-ranked, pairwise feature sets obtained after the first stage of the training algorithm. The sets are sorted in descending order based on the column $N_{i_1} + N_{i_1,i_2}$ which represents the number of cases correctly classified (excluded) using thresholds on the joint feature pairs f_{i_1} and f_{i_2}. If two sets have the same value of jointly excluded cases, the number of the cases excluded by only the first feature is used for sorting then the number of the cases excluded by the second feature. This is to give more priority to the feature f_{i_1} so as to get minimal number of features.

From Table III, it can be seen that almost 79% of the events can be classified at this first stage (5130 out of 6500 events). This validates our original motivation that the DTL would be able to discriminate between most islanding or non-islanding events within a very short period of time ($10ms$).

The structures of the DTLs produced using the proposed training algorithm are shown in Fig. 8 (a, b, c, and d) for feature sets of size 1, 2, 3 and 4 respectively. The values presented in Fig. 8 are the upper and lower limits of the features which were extracted using the proposed DTL algorithm. As can be seen, the produced DTL classifiers vary somewhat in size and the features selected. When only one feature per time window is used, the resulting tree has 5 decision levels. This is because the predictive capability of one feature is less than that of a combination of two or more features, which necessitates the use of more stages. However, the tree produced using subsets of size 4 is composed of 5 level of rules, though these are contained within two DTL stages. This points to a tradeoff between the complexity of each layer, determined by the number of decision rules used, and the time taken to correctly classify a case, which is a function of the number of stages in the DTL. More studies are needed to determine the optimum balance but in general, having some "tunability" in the system was perceived to be a good thing as it suggests that the proposed approach can be customized to suit different applications and requirements.

It can also be observed that the trees which use 2, 3, and 4 feature subsets have the same root node THD_V, and the trees which use 3 and 4 feature subsets share a common set of features for the first three levels, which were THD_V, δV_+ and δF. From this we can infer that this group of features has the best predictive capability at this time scale. It can also be noticed, from Fig. 8(c) and (d), that the DTL needs only one feature in the $10 - 20ms$ window to classify the remaining cases, even though it is allowed to have up to 3 and 4 features respectively.

Another interesting observation can be made by comparing the trees depicted in Fig. 8(b) and (d). Here, it can be seen that in tree (b), four features are used: two of which were

TABLE III
THE NUMBER OF CASES CLASSIFIED BY SETS OF TWO FEATURES OUT OF 6,500 CASES

f_{i_1}	f_{i_2}	$N_{i_1} + N_{i_1,i_2}$	N_{i_1}	N_{i_1,i_2}
THD_V	δQ	5130	1624	3506
THD_V	δV	4816	1624	3192
THD_V	δV_+	4626	1624	3002
V_+	δF	4493	2880	1613
δV	δV_+	4293	2520	1773
δV_+	δV_-	4264	3086	1178
V_+	δP	4237	2880	1357
V	δV_0	4066	2859	1207
δV_+	δV_0	4008	3086	922
V	δF	3939	2859	1080

TABLE IV
FEATURE SETS AND CLASSIFICATION ERROR WHEN USING DIFFERENT SUBSETS OF DATA FOR BUILDING THE TREES

Feature set size	10%	20%	30%	40%	50%
1	δV_+ δV_- V_- V_- F	δV_+ δV_- V_- F V_-	δV_+ δV_- V_- F V	δV_+ δV_- V_- F V	δV_+ δV_- V_- F V_-
Error (%)	0.69%	0.25%	0.07%	0.02%	0.02%
2	THD_V δQ F δQ	THD_V δQ Q δV_-	THD_V δQ δTHD_V δV_-	THD_V δQ δTHD_V δV_-	THD_V δQ δTHD_V δV_-
Error (%)	0.17%	0.26%	0.01%	0.00%	0.02%
3	THD_V δV_+ V_- δQ	THD_V δV_+ δF δQ	THD_V δV_+ δF δQ	THD_V δV_+ δF δQ	THD_V δV_+ δF δQ
Error (%)	0.08%	0.05%	0.05%	0.05%	0.06%
4	THD_V δV_+ δF δV_- Q	THD_V δV_+ δF δV_- δQ	THD_V δV_+ δF δV_- δQ	THD_V δV_+ δF δV_- δQ	THD_V δV_+ δF δV_- δQ
Error (%)	0.51%	0.22%	0.05%	0.05%	0.02%

extracted from the $0-10ms$ window and the other two from the $10-20ms$ window; tree (d), on the other hand, uses four features extracted from the $0-10ms$ window but these are incapable of classifying all the cases and a fifth feature is required from the $20ms$ window. This clearly shows the time dependant nature of the best feature vector combination. It is worth noting that the number of training cases detected within $20ms$ for subsets of one, two, three and four features are 3096, 5103, 5893 and 6363 respectively. Hence, using four features per stage allows the detection of more cases in less time but at the cost of greater complexity per stage and lower accuracy as will be explained in the next section.

B. Case II: Training set size

System disturbances are included during the simulation stage. Hence, the set of simulated cases includes many system normal and abnormal conditions that can occur in real power systems and accounted for during the selection of the boundaries. Therefore to study the robustness of the algorithm, random subsets consisting of 10%, 20%, 30%, 40%, and 50% of the total number of the simulated cases were chosen to be utilized for extracting the prominent feature groups and their boundaries while the rest of the cases are used for testing.

The feature sets used and classification errors of the resulting decision trees are shown in Table IV. As can be seen there are slight changes in the feature sets obtained using the different sizes of training sets. Fig. 10 shows the errors corresponding to each feature subset size and data subset. For all combinations there were small numbers of misclassified cases but the misclassification rates were invariably very low ($> 1\%$ for all cases, and $> 0.1\%$ in 14 out of 20 cases). In addition, as expected the classification errors were broadly lower when larger training sets were used, as a result of better coverage of the possible test cases. However, this cannot be guaranteed for all instances and there are some exceptions (for the combinations of 50% training set size with feature set sizes

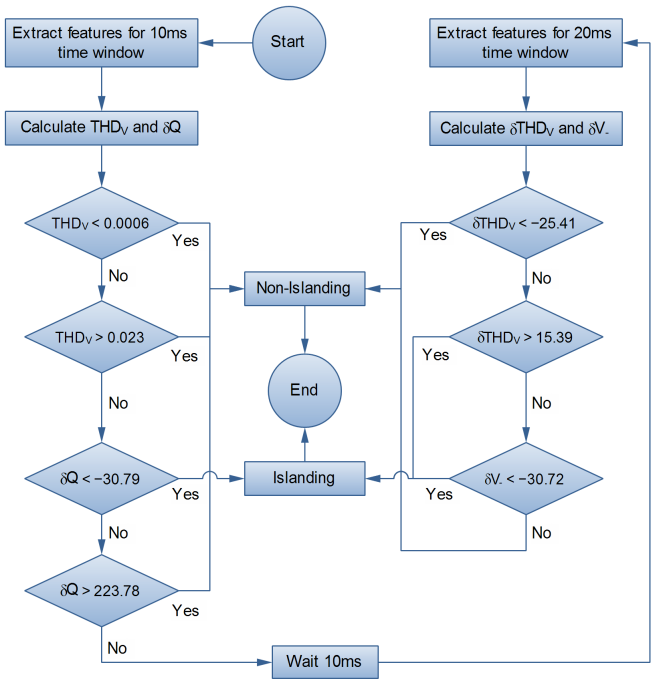

Fig. 9. Flowchart of the proposed method considering two features per stage (tree (b) in Fig. 8)

of 2 and 3); in both instances, the increases are very small and amount to only 1 or 2 misclassified cases out of thousands of test cases.

Feature sets of sizes 2 and 3 achieved lower classification errors, averaging 0.092% and 0.058% respectively while feature sets of sizes 1 and 4 had 0.21% and 0.17% misclassification rates respectively. Even though all four cases considered gave reasonably good accuracy for the various data set sizes, which shows the robustness of the proposed method, the selection of feature set size per time window depends on the test system under consideration.

For training set size of 50%, for the two-feature per stage, there are two misclassified cases; one islanding and one non-islanding cases. For the three-feature per stage, there is one islanding case and two non-islanding cases that were misclassified. It is worthy to note that those misclassified cases are out of 12995 cases (5906 islanding and 7086 non-islanding). The training set was chosen randomly but it has been found that further improvement can be achieved if the misclassified cases are included in the training stage. To prove this, the inclusion of the aforementioned misclassified cases in the training set produced updated δQ and δTHD_V threshold values which subsequently resulted in 100% classification accuracy. Thus, the proposed method has a considerably very small (almost negligible) NDZ comparable to the methods reported in [15] and [16].

Fig. 9 presents the flowchart of the proposed method considering two features per stage. The first stage (first $10ms$) includes the calculation of features THD_V and δQ and setting thresholds on both parameters. Islanding cases that are not detected in the first stage are passed to the second stage which includes the calculation of features δTHD_V and δV_-. Those features are calculated based on a $20ms$ window size where

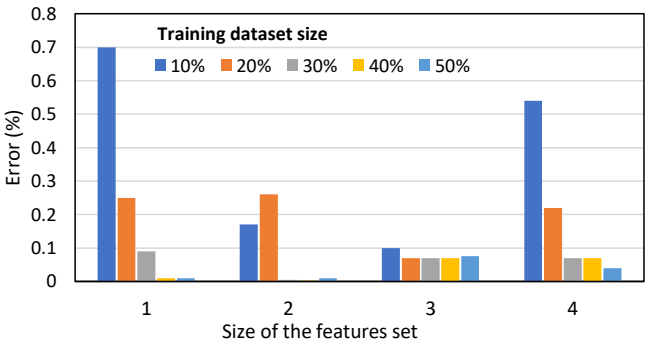

Fig. 10. Classification error at different feature sets and training dataset size. Using two features and a training dataset of size 40%, the proposed method was able to achieve zero classification error.

thresholds are set on those features for islanding detection.

Islanding detection methods have been proposed in the literature for either synchronous or inverter-based DG. Each type of DG performs differently during an islanding condition. For example, with an inverter-based DG, the reactive power mismatches is primarily responsible for frequency deviations [31]. On the contrary, the frequency during an islanding condition with synchronous-based DG will deviate depending on the active power mismatch [32]. In addition, the interface control of each type is different and some islanding detection methods such as SFS that are applicable to inverter-based DG are not applicable to synchronous-based [33]. For this reason, this paper focuses on developing an efficient islanding detection method for synchronous-based DG only.

C. Case III: Impact of inverter-based DG interconnection

The proposed algorithm is further tested to examine the impact of inverter-based DG interconnection on the proposed islanding detection method as such modification is considered a major change in the distribution system.

inverter-based DG can be equipped with either active or passive islanding detecting methods. It is worthy to mention that inveter based DG equipped with active islanding detection methods will further enhance the islanding detection capabilities since those methods rely on forcing a drift in either frequency and voltage. To consider a harder case, in this study, the inverter-based DG is assumed to be equipped with a passive method that relies on voltage and frequency relays. A 500 kVA inverter-based DG is connected in parallel with a 500 kVA synchronous-based DG. A total of 100 islanding cases are simulated and tested on a DT with two features per stage. The classification accuracy is 95% when using training set that does not include any cases involving inverter-based DG which is expected for a learning-based approach to have lower accuracy. Furthermore, the accuracy was enhanced to 100% after including those new cases in the training set without jeopardizing the overall accuracy.

In light of such result we conclude that although the DT was not trained on a system configuration with inverted based DG but still it shows good results. Including this new configuration in the training set enhanced the DT performance.

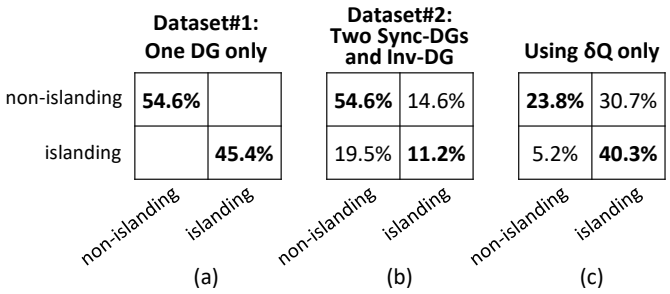

Fig. 11. Comparing the classification results of using the proposed method on a system with (a) one Sync-DG, and (b) two Sync-DGs and one Inv-DG. Results in (c) are for using only δ Q for islanding detection.

D. Case IV: Impact of synchronus-based DG

In this case study, an intricate scenario of having another synchronous DG connected in the network is examined to evaluate the performance of the proposed islanding detection method.

Towards this end, in addition to the 500 kVA synchronous DG and 500 kVA inverter-based DG both connected at bus 848, another 500 kVA synchronous DG is connected to the network at bus 832. A total of 205 islanding and non-islanding cases are simulated and the signals are stored as dataset#2. Using dataset#1, which corresponds to the previously simulated cases on the network with only one synchronous DG connected, a DT with two features per stage is trained. The performance of the DT is then tested on dataset#2 and the results are shown in Fig. 11 as two confusion matrices. The figure indicates that the 100% classification accuracy in Fig. 11-(a) achieved using dataset#1 has dropped to approximately 65.8% in Fig. 11-(b) when the DT tested on dataset#2. This is because the training set that does not include any cases involving two DGs which is expected for a learning-based approach to have lower accuracy. However, using samples from both dataset#1 and dataset#2 to train the DT, the accuracy was enhanced to 100%.

E. Discussion

Islanding detection is a protection requirement for DG and it is important while designing resilient and reliable distribution systems to develop an islanding detection method that is capable of distinguish between normal system disturbances and islanding events.

The rate of change of reactive power has been proposed for synchronous based DGs in [34]. However, this method relies **only** on the rate of change of reactive power, whereas the proposed multi-stage islanding detection method relies on multiple features as in [15] and [35], and also determines the optimal features and their thresholds for each time window (stage). This allows for timely and accurate islanding detection. Many islanding events can be detected in the first stage (i.e., after 10 msec), while in the second stage (i.e., after 20 msec) more difficult cases are detected. The proposed method has been compared with the rate of change of reactive power where the same approach was utilized but considering only the rate of change of reactive power as the only available feature

and only one stage (20 msec). For a 20 msec detection time, Fig. 11-(a) and (c) presents a comparative analysis highlighting both the accuracy of the proposed method as well as the rate of change of reactive power method. As can been seen, the classification accuracy has dropped from 100% to 69.1% using the rate of change of reactive power method for a 20 msec time window and thus the proposed approach has negligible NDZ.

Considering the islanding events, the proposed method is capable of detecting 72.6% of the cases in 10 msec (first stage) and the rest in 20 msec (second stage). This detection time is less than the times 100 msec, 104 msec, and 200 msec reported in [34], [36], and [37], respectively.

It is worthy to note that the concept of multistage islanding detection can be further extended by including features such as the phase angle, individual current harmonics and their rate of changes which can be considered for future work.

The proposed islanding detection method is suitable for synchronous-based DG. For inverter-based DG, the proposed multi-stage islanding detection concept can be applied but due to the difference between the two DG type characteristics, a new feature set would need to be determined for inverter-based DG which is out of the scope of this paper and can be considered for future work. The proposed islanding detection method is implemented at each DG location and thus does not require communication.

V. Conclusion

In this paper a novel, multistage islanding detection approach based on the decision tree-like classifier is proposed and tested on a system which incorporates a synchronous-based DG. The proposed islanding detection approach was tested on a standard IEEE 34-bus radial distribution test system with a variety of disturbances. In this passive islanding detection approach, each stage uses a different feature set collected over a range of time windows for detecting and distinguishing between islanding and non-islanding events. The results indicate that the use of multiple features in the detection method is more effective when different time windows are considered for the various groups of features to reduce the NDZ. The proposed method has also been tested for systems with both inverter and synchronous-based DG and it has been shown that the proposed method has negligible NDZ. The best features to be used for each detection stage will depend on the chosen window size and thus finding the optimal window size can be considered for future work. In addition, the interaction between multiple synchronous-based DG and its effect on the feature selection may require further investigations. While the IEEE 1547 standard specifies a detection time below 2 seconds, any method which is able to further reduce the detection time is an improvement since there may be unforeseen situations which are not represented in the current training or testing set. In such situations, having as larger time "buffer" as possible is clearly valuable as long as it does not add further complexity to the system. Furthermore, the proposed approach simplifies the decision process since many cases are classified immediately after observing only one or two features.

References

[1] P. K. Ganivada and P. Jena, "Active slip frequency based islanding detection technique for grid-tied inverters," *IEEE Transactions on Industrial Informatics*, vol. 16, no. 7, pp. 4615–4626, 2020.

[2] S. Murugesan and V. Murali, "Decentralised unintentional islanding identification for converter interfaced multiple dgs," *IEEE Transactions on Industrial Informatics*, p. early access, 2020.

[3] S. Murugesan and V. Murali, "Hybrid analyzing technique based active islanding detection for multiple dgs," *IEEE Transactions on Industrial Informatics*, vol. 15, no. 3, pp. 1311–1320, 2019.

[4] T. Funabashi, K. Koyanagi, and R. Yokoyama, "A review of islanding detection methods for distributed resources," in *Power Tech Conference Proceedings, 2003 IEEE Bologna*, vol. 2, p. 6, Jun. 2003.

[5] W. Bower and M. Ropp, "Evaluation of Islanding Detection Methods for Photovoltaic Utility Interactive Power Systems," tech. rep., IEA, 2002.

[6] J. Vieira, W. Freitas, W. Xu, and A. Morelato, "Efficient coordination of ROCOF and frequency relays for distributed generation protection by using the application region," *Power Delivery, IEEE Transactions on*, vol. 21, pp. 1878–1884, Oct. 2006.

[7] M. Redfern, J. Barrett, and O. Usta, "A new loss of grid protection based on power measurements," in *Developments in Power System Protection, Sixth International Conference on (Conf. Publ. No. 434)*, pp. 91–94, Mar. 1997.

[8] A. Samui and S. Samantaray, "Assessment of rocpad relay for islanding detection in distributed generation," *Smart Grid, IEEE Transactions on*, vol. 2, pp. 391–398, Jun. 2011.

[9] F.-S. Pai and S.-J. Huang, "A detection algorithm for islanding-prevention of dispersed consumer-owned storage and generating units," *Energy Conversion, IEEE Transactions on*, vol. 16, pp. 346–351, Dec. 2001.

[10] W. Freitas, W. Xu, C. Affonso, and Z. Huang, "Comparative analysis between ROCOF and vector surge relays for distributed generation applications," *Power Delivery, IEEE Transactions on*, vol. 20, pp. 1315–1324, Apr. 2005.

[11] S.-I. Jang and K.-H. Kim, "An islanding detection method for distributed generations using voltage unbalance and total harmonic distortion of current," *Power Delivery, IEEE Transactions on*, vol. 19, pp. 745–752, Apr. 2004.

[12] P. Ray, N. Kishor, and S. Mohanty, "Islanding and power quality disturbance detection in grid-connected hybrid power system using wavelet and s -transform," *Smart Grid, IEEE Transactions on*, vol. 3, pp. 1082–1094, Sept. 2012.

[13] W. K. A. Najy, H. H. Zeineldin, A. H. K. Alaboudy, and W. L. Woon, "A Bayesian Passive Islanding Detection Method for Inverter-Based Distributed Generation Using ESPRIT," *Power Delivery, IEEE Transactions on*, vol. 26, pp. 2687–2696, Oct. 2011.

[14] M. Padhee, P. Dash, K. Krishnanand, and P. Rout, "A fast gauss-newton algorithm for islanding detection in distributed generation," *Smart Grid, IEEE Transactions on*, vol. 3, pp. 1181–1191, Sept. 2012.

[15] K. El-Arroudi, G. Joos, I. Kamwa, and D. McGillis, "Intelligent-Based Approach to Islanding Detection in Distributed Generation," *Power Delivery, IEEE Transactions on*, vol. 22, pp. 828–835, Apr. 2007.

[16] N. Lidula, N. Perera, and A. Rajapakse, "Investigation of a fast islanding detection methodology using transient signals," in *Power Energy Society General Meeting, 2009. PES '09. IEEE*, pp. 1–6, Jul. 2009.

[17] S. Kar and S. Samantaray, "Data-mining-based intelligent anti-islanding protection relay for distributed generations," *Generation, Transmission & Distribution, IET*, vol. 8, pp. 629–639, Apr. 2004.

[18] M. Alam, K. Muttaqi, and A. Bouzerdoum, "An Approach for Assessing the Effectiveness of Multiple-Feature-Based SVM Method for Islanding Detection of Distributed Generation," *Industry Applications, IEEE Transactions on*, vol. 50, pp. 2844–2852, July.-Aug. 2014.

[19] B. Matic-Cuka and M. Kezunovic, "Islanding Detection for Inverter-Based Distributed Generation Using Support Vector Machine Method," *Smart Grid, IEEE Transactions on*, vol. 5, pp. 2676–2686, Nov. 2014.

[20] S. Mohanty, N. Kishor, P. Ray, and J. Catalao, "Comparative Study of Advanced Signal Processing Techniques for Islanding Detection in a Hybrid Distributed Generation System," *Sustainable Energy, IEEE Transactions on*, vol. 6, pp. 122–131, Jan. 2015.

[21] S. Alshareef, S. Talwar, and W. Morsi, "A New Approach Based on Wavelet Design and Machine Learning for Islanding Detection of Distributed Generation," *Smart Grid, IEEE Transactions on*, vol. 5, pp. 1575–1583, Jul. 2014.

[22] H. R. Baghaee, D. Mlakić, S. Nikolovski, and T. Dragičević, "Support vector machine-based islanding and grid fault detection in active dis-

tribution networks," *IEEE Journal of Emerging and Selected Topics in Power Electronics*, 2019.

[23] D. Mlakić, H. R. Baghaee, and S. Nikolovski, "A novel anfis-based islanding detection for inverter-interfaced microgrids," *IEEE Transactions on Smart Grid*, vol. 10, no. 4, pp. 4411–4424, 2018.

[24] R. Bekhradian, M. Davarpanah, and M. Sanaye-Pasand, "Novel Approach for Secure Islanding Detection in Synchronous Generator Based Microgrids," *IEEE Transactions on Power Delivery*, vol. 34, no. 2, pp. 457–466, 2018.

[25] P. Kundur, N. Balu, and M. Lauby, *Power system stability and control*. The EPRI power system engineering series, McGraw-Hill, 1994.

[26] IEEE, "IEEE Standard for Interconnecting Distributed Resources With Electric Power Systems," *IEEE Std 1547-2003*, pp. 1–28, July 2003.

[27] P. Mahat, Z. Chen, and B. Bak-Jensen, "A hybrid islanding detection technique using average rate of voltage change and real power shift," *Power Delivery, IEEE Transactions on*, vol. 24, pp. 764–771, Apr. 2009.

[28] J. Vieira, W. Freitas, W. Xu, and A. Morelato, "Performance of frequency relays for distributed generation protection," *Power Delivery, IEEE Transactions on*, vol. 21, pp. 1120–1127, Jul. 2006.

[29] J. Vieira, D. Correa, W. Freitas, and W. Xu, "Performance curves of voltage relays for islanding detection of distributed generators," *Power Systems, IEEE Transactions on*, vol. 20, pp. 1660–1662, Aug. 2005.

[30] W. El-Khattam, A. Yazdani, T. Sidhu, and R. Seethapathy, "Investigation of the local passive anti-islanding scheme in a distribution system embedding a pmsg-based wind farm," *Power Delivery, IEEE Transactions on*, vol. 26, pp. 42–52, Jan. 2011.

[31] Z. Ye, A. Kolwalkar, Y. Zhang, P. Du, and R. Walling, "Evaluation of anti-islanding schemes based on nondetection zone concept," *Power Electronics, IEEE Transactions on*, vol. 19, no. 5, pp. 1171–1176, 2004.

[32] W. Freitas, W. Xu, C. M. Affonso, and Z. Huang, "Comparative analysis between rocof and vector surge relays for distributed generation applications," *Power Delivery, IEEE Transactions on*, vol. 20, no. 2, pp. 1315–1324, 2005.

[33] D. Finney, B. Kasztenny, and M. Adamiak, "Generator protection needs in a DG environment," tech. rep., GE Power Management, GER-4003, 2002.

[34] S. Nikolovski, H. R. Baghaee, and D. Mlakić, "Islanding Detection of Synchronous Generator-Based DGs using Rate of Change of Reactive Power," *IEEE Systems Journal*, vol. 13, no. 4, pp. 4344–4354, 2019.

[35] K. El-Arroudi and G. Joos, "Data Mining Approach to Threshold Settings of Islanding Relays in Distributed Generation," *IEEE Transactions on power systems*, vol. 22, no. 3, pp. 1112–1119, 2007.

[36] M. B. R. Noroozian, "Reactive Power Based Anti-Islanding Scheme for Synchronous Distributed Generators," *International Journal on "Technical and Physical Problems of Engineering*, no. 13, pp. 30–37, 2012.

[37] S. Raza, H. Arof, H. Mokhlis, H. Mohamad, and H. A. Illias, "Passive Islanding Detection Technique for Synchronous Generators Based on Performance Ranking of Different Passive Parameters," *IET Generation, Transmission & Distribution*, vol. 11, no. 17, pp. 4175–4183, 2017.